PERSPECTIVE

Guidelines for Imaging the Choriocapillaris Using OCT Angiography

ZHONGDI CHU, QINQIN ZHANG, GIOVANNI GREGORI, PHILIP J. ROSENFELD, AND RUIKANG K. WANG

• PURPOSE: To provide guidance on how to appropriately quantitate various choriocapillaris (CC) parameters with optical coherence tomography angiography (OCTA).
• DESIGN: Evidence-based perspective.
• METHODS: Review of literature and experience of authors.
• RESULTS: Accurate and reliable quantification of CC using OCTA requires that CC can be visualized and that the measurements of various CC parameters are validated. For accurate visualization, the selected CC slab must be physiologically sound, must produce images consistent with histology, and must yield qualitatively similar images when viewing repeats of the same scan or scans of different sizes. For accurate quantification, the measured intercapillary distances (ICDs) should be consistent with known measurements using histology and adaptive optics and/or OCTA, the selected CC parameters must be physiologically and physically meaningful based on the resolution of the instrument and the density of the scans, the selected algorithm for CC binarization must be appropriate and generate meaningful results, and the CC measurements calculated from multiple scans of the same and different sizes should be quantitatively similar. If the Phansalkar local thresholding method is used, then its parameters must be optimized for CC based on the OCTA instrument and scan patterns used. It is recommended that the window radius used in the Phansalkar method should be related to the expected average ICD in normal eyes.
• CONCLUSIONS: Quantitative analysis of CC using commercially available OCTA instruments is complicated, and researchers need to tailor their strategies based on the instrument, scan patterns, anatomy, and thresholding strategies to achieve accurate and reliable measurements. (Am J Ophthalmol 2021;222:92–101. © 2020 Elsevier Inc. All rights reserved.)

Accepted for publication Aug 28, 2020.

From the Department of Bioengineering, University of Washington, Seattle, Washington USA (Z.C., Q.Z., R.K.W.); Department of Ophthalmology, Bascom Palmer Eye Institute, University of Miami Miller School of Medicine, Miami, Florida, USA (G.G., P.J.R.); and Department of Ophthalmology, University of Washington, Seattle, Washington, USA (R.K.W.).

Inquiries to Ruikang K. Wang, University of Washington, Box 355061, 3720 15th Ave NE, Seattle, Washington 98195-5061, USA; e-mail: wangrk@uw.edu

THE IMAGING AND ANALYSIS OF THE CHORIOCAPILLARIS (CC) using optical coherence tomography angiography (OCTA) has become one of the hottest topics in ophthalmological research in recent years. Researchers have used different OCTA instruments and various analytical methods to characterize various properties of the CC in ocular diseases, such as age-related macular degeneration,[1] diabetic retinopathy,[2] glaucoma,[3] and central serous chorioretinopathy.[4] Like many new techniques, the emergence of CC imaging and its quantitation has been accompanied by new challenges due to limited understanding of current technology and the inappropriate use of various algorithms. Many of the limitations and challenges associated with these strategies have been explored,[5–7] but no definitive conclusions or protocols have been provided to guide researchers on how to best image the CC and to perform its quantitative analysis. This report aims to summarize lessons we learned in our experience and to provide evidence-based guidelines on how to appropriately image and analyze the CC flow using OCTA, with a particular emphasis on swept source OCTA (SS-OCTA).

ACCURATE CC VISUALIZATION USING OCTA

THE FIRST STEP IN APPROPRIATELY ANALYZING THE FLOW within the CC is to accurately visualize the CC. The CC is a thin but dense vascular monolayer located along the inner choroid, adjacent to the Bruch membrane (BM). The most important step in visualizing the CC flow using OCTA is an accurate segmentation of the relevant retinal structures.

• CC SLAB SELECTION MUST BE PHYSIOLOGICALLY SOUND: OCT is an imaging modality that provides cross-sectional, depth-encoded information. Therefore, in OCT and OCTA imaging, the *z*-axis (depth) segmentation is the first step in visualizing any particular layer of interest.

0002-9394/$36.00
https://doi.org/10.1016/j.ajo.2020.08.045

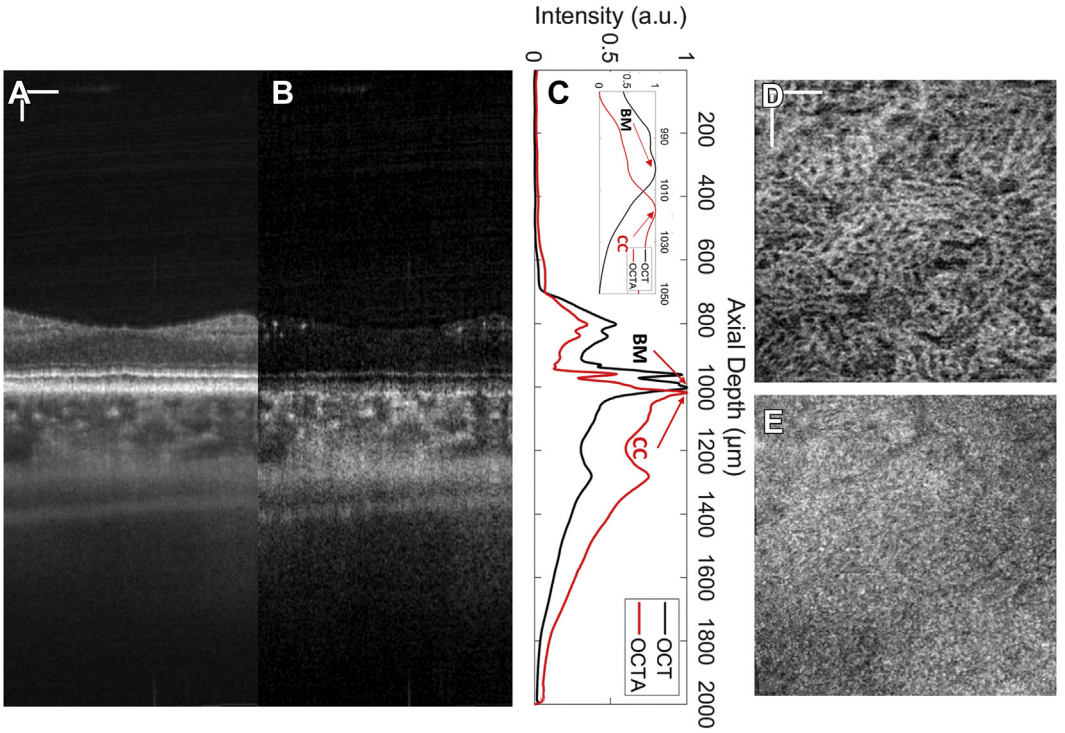

FIGURE 1. Illustration of how to define the choriocapillaris (CC) slab by averaging all A-lines in both swept-source optical coherence tomography (SS-OCT) volume and SS-OCT angiography (SS-OCTA) volume datasets using a previously published high-resolution (~7 μm laterally, compared with ~16-20 μm in commercial OCT systems) SS-OCT system.[13] (A) Representative SS-OCT B-scan and (B) corresponding OCTA B-scan. (C) Averaged A-line profiles from SS-OCT (black) and SS-OCTA (red) signals, with the zoomed-in profile near the CC in the top right corner. The OCT peak at 1,002 μm represents the BM, the OCTA peak at 1,018 μm represents the posterior boundary of the CC. (D) *En face* OCTA CC image with the slab positioned at a depth of 1,004−1,020 μm. (E) *En face* OCT CC image of the same slab from (D). Scale bars represent 100 μm.

Traditionally, volumetric OCT data have been used to perform layer segmentation because different ocular layers often have different OCT reflectivity due to their specific optical properties.[8] In the case of CC visualization, the theoretical definition of the CC slab should start from its anatomic location, which is adjacent to the outer boundary of BM and has the thickness of a single capillary diameter.[9]

Ideally, the thickness of the CC slab should be equal to the axial diameter of a single CC vessel, which decreases with aging, with a mean thickness of 9.8 μm in the first decade of life and 6.5 μm in the tenth decade of life.[10] However, the convolutional effect of OCT resolution will artificially fatten the biological features during imaging. Therefore, the thickness of the CC slab should take into account the effects of axial resolution of OCT (~6 μm). Thus, a CC slab of 10-20 μm thickness, located directly beneath the BM, should yield the best OCTA *en face* images. In practice, due to the limited axial resolution of OCTA (~6 μm) and the scattering properties of these retinal layers, common OCT systems cannot individually resolve the retinal pigment epithelium (~11 μm thick) from the BM (~2-6 μm thick in normal eyes),[10,11] unless they are separated due to pathology. Thus, in normal eyes, the retinal pigment epithelium/BM complex is generally presented as a wide bright band in the OCT image, and the CC slab should be defined parallel to the segmentation line of either the retinal pigment epithelium or BM. If the retinal pigment epithelium is being segmented (upper boundary of the retinal pigment epithelium/BM complex), the CC slab should be placed approximately 16 μm beneath the segmentation line, considering the thickness of the retinal pigment epithelium and BM. If the BM is being segmented (the lower boundary of the retinal pigment epithelium/BM complex), the CC slab should be placed approximately 4 μm below the segmentation line, considering the thickness of BM. Another approach to define the CC slab could use the averaged A-lines as previously described by multiple groups.[12–14] Figure 1 shows an example of such approach. Figure 1, A and B are OCT and OCTA B-scans, respectively, from previously published high-resolution (~7 μm laterally, compared with ~16-20 μm in commercial OCT systems) SS-OCT data.[13] Figure 1, C shows the averaged A-line profiles through the whole volume. Two obvious peaks can be observed, 1 from the OCT data and 1 from the OCTA data, labeled with arrows. The peak from the

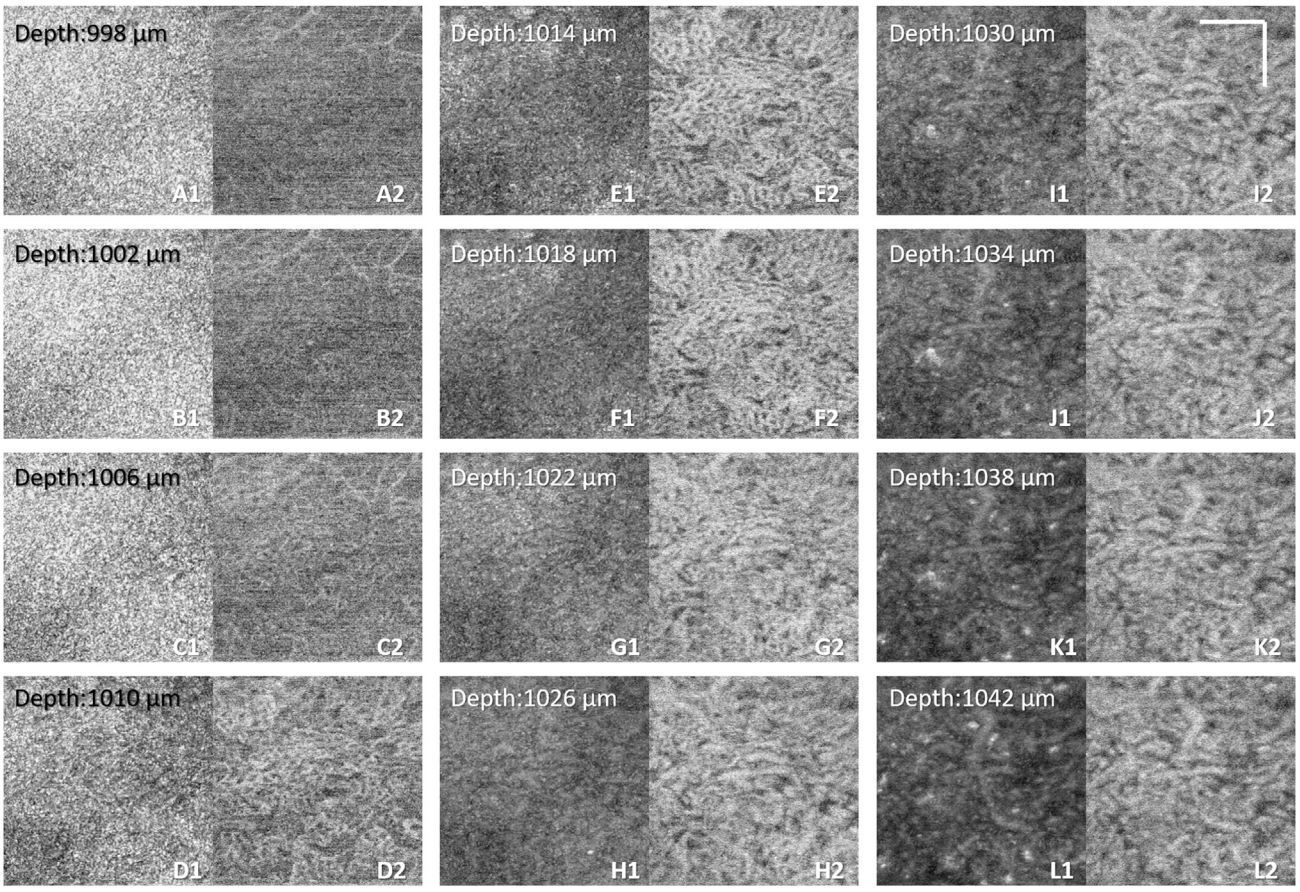

FIGURE 2. Example showing the appearances of *en face* swept-source optical coherence tomography (SS-OCT) and SS-OCT angiography (SS-OCTA) images at different depth positions of the same dataset in Figure 1. (A1-L1) Single pixel *en face* OCT images at depth position of 998-1,042 µm, position 1,002 µm is the calculated Bruch membrane position, as shown in Figure 1. (A2-L2) Single pixel *en face* OCTA images at depth position of 998-1,042 µm, position 10,018 µm is the calculated choriocapillaris posterior boundary position, as shown in Figure 1. Scale bars represent 100 µm.

OCT data represents the BM (positioned at 1,002 µm depth), whereas the peak from the OCTA data represents the posterior boundary of the CC (positioned at 1,018 µm depth). Figure 2 shows the *en face* OCT and OCTA images at each depth position (single pixel). With this approach, the posterior boundary of the CC slab can be decided by identifying the CC peak from averaged OCTA A-lines, and the anterior boundary of the CC slab can be decided by identifying the BM peak from the averaged OCT A-lines. Figure 1, D (OCTA) and Figure 1, E (OCT) show such a CC slab positioned from 4 µm below the BM peak to the CC posterior boundary peak.

When generating CC slabs, researchers should always take OCT CC structure *en face* images into consideration; these structural images can be used to judge if the CC slab is too deep into the choroid. For example, Figure 3 shows an example of a normal eye acquired by PLEX Elite 9000 (Carl Zeiss Meditec, Dublin, California, USA), in which different OCT and OCTA CC slabs were extracted using different locations offset to the BM segmentation line (manual segmentation, red dashed lines in Figure 3, A and B). Although the OCTA CC *en face* flow images look similar across different slabs, the changes in the appearance of the OCT structural CC *en face* images are apparent, ranging from a homogeneous appearance to a variegated appearance. Researchers should be aware that if the OCT structural CC *en face* image appears variegated, as in Figure 3, D and F, then your CC slab is too deep into the choroid. This could also be seen in data scanned from our lab-built, high-resolution SS-OCT system, in which Figure 2, G1-L2 clearly demonstrates that the variegated OCT structural images indicate that the slab is placed too deep into the choroid rather than at the real CC. It could be observed that the choroidal slabs in Figure 2, K1 and K2 show larger diameter vasculature in the OCTA image and variegated pigment appearances in the OCT image, whereas the CC slabs in Figure 2, E1 and E2 show smaller diameter vasculature in the OCTA image and homogenous appearance in the OCT image.

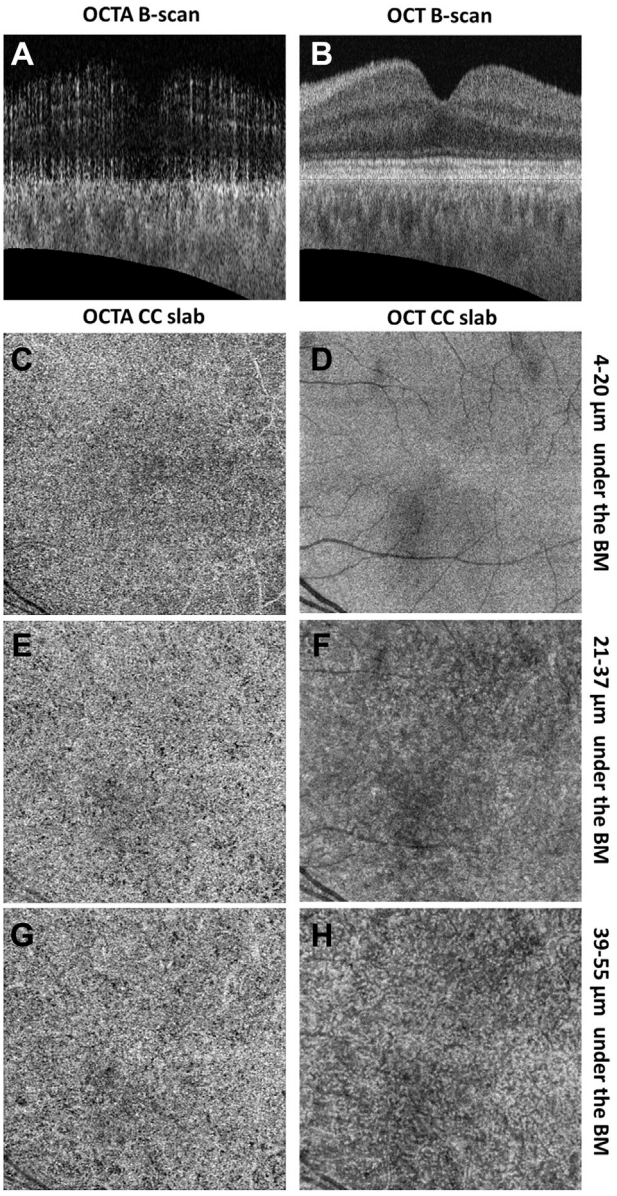

FIGURE 3. Example of PLEX Elite 9000 swept-source optical coherence tomography angiography (SS-OCTA) choriocapillaris (CC) slab with a thickness of 15 µm located at selected positions of a 6 × 6-mm scan in a normal eye. (A and B) Cross-sectional SS-OCTA and SS-OCT B-scans showing the position of segmented Bruch membrane (BM) (red dashed lines). (C and D) *En face* SS-OCTA and SS-OCT CC images with a position of 4-20 µm under the segmented BM. (recommended) (E and F) *En face* SS-OCTA and SS-OCT CC images with a position of 21-37 µm under the segmented BM. (G and H) *En face* SS-OCTA and SS-OCT CC images with a position of 39-55 µm under the segmented BM. OCTA CC images were compensated for shadowing effect by using the CC structural signals, and retinal projection artifacts were removed. Positions in micrometers have been rounded (1 pixel = 1.9531 µm).

Because not all research groups develop their own segmentation software to generate *en face* images, it is common for researchers to rely on the proprietary segmentation software in each commercial OCT instrument to generate *en face* OCT and OCTA images. Therefore, it is important to check and correct all segmentation lines, especially in the presence of pathology because current automated segmentation algorithms can often be unreliable, especially along the retinal pigment epithelium/BM layer.

• **SELECTED CC SLAB MUST SHOW SIMILARITY IN APPEARANCE COMPARED WITH HISTOLOGY:** Once the anatomically correct CC slab is generated, the corresponding OCTA CC *en face* flow image should be visually checked for resemblance to previously published histological images. Previous studies showed that the CC network has distinguishable morphological features at different regions.[15] In the submacular region, the CC appears as a dense meshwork pattern of interconnected capillaries separated by septa, whereas in the equatorial and peripheral regions, the CC has a lobular pattern in which arterioles and venules join the segment from either the center or the periphery of the lobules. The averaged CC vessel diameter (laterally) under the macular was reported as 16-20 µm, with intercapillary distances (ICDs) of 5-20 µm. However in the equatorial region, CC vessel diameter (laterally) was reported as 20-50 µm with ICDs of 50-200 µm.[16]

As previously explained,[5] the CC networks under the macula cannot be fully resolved due to the limited lateral resolution of OCTA, but more widely spaced capillary networks within the equatorial regions are easier for OCTA to resolve. Registering and averaging multiple OCTA volumes is one useful approach for improving CC visualization, but averaging does not improve the optical resolution of the images. Therefore, individual capillaries will still be beyond the instrument's reach.[17] Researchers should consider averaging images to visually confirm the resemblance of their OCTA CC images with histological images, particularly in the peripheral regions. Although some of the capillaries within the macula will still remain unresolved, pathological flow deficits will be better defined due to a decrease in noise. Figure 4 demonstrates one such example in which average OCTA CC images (previously published data[17]) show a high degree of similarity compared with scanning electron microscope images.[16] With this comparison, researchers can increase their confidence that the OCTA signals they are looking at are from the CC networks.

• **REPEATED SCANS OF SAME AND DIFFERENT SIZES SHOULD BE QUALITATIVELY SIMILAR:** In addition to comparing CC images with histological CC images, researchers should also collect data to confirm that repeated scans of the same subject, using the same scanning pattern, are qualitatively similar. Moreover, when performing

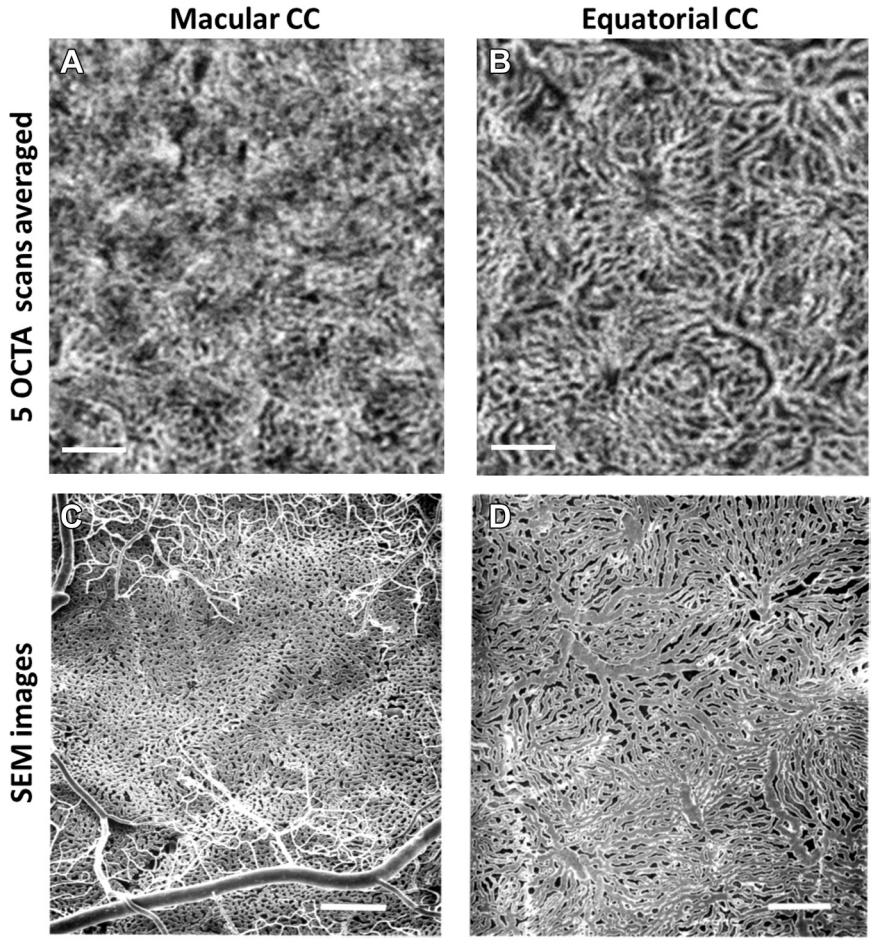

FIGURE 4. Comparison of choriocapillaris (CC) in the macular region and equatorial region using PLEX Elite 9000 swept-source optical coherence tomography angiography (SS-OCTA) and scanning electron microscopy (SEM). (A) *En face* SS-OCTA CC image acquired in the macular region, 5 3 × 3-mm scans averaged with 300 A-scans and 300 B-scan positions. (B) *En face* SS-OCTA CC image acquired in the equatorial region, 5 scans averaged (as previously described). (C) SEM CC image of methyl methacrylate casts under the macular region, reproduced from Olver[16] with permission. (D) SEM CC image of corrosion casts under the equatorial region, reproduced from Olver[16] with permission.

repeated scans of the same subject at the same location using different scanning patterns (such as 3 × 3-mm scans and 6 × 6-mm scans), researchers should confirm that these scans are qualitatively similar. The next step in generating OCTA CC images requires that the researcher should also consider the physical limitations of OCT imaging, particularly the potential for artifacts. For example, in cases of pathology, especially in the presence of drusen, the OCT signal can be significantly attenuated after passing through drusen. As a result, the OCTA flow signal, derived from the OCT structural signal, often shows abnormally low intensity. A specially designed compensation strategy[18] is helpful in such cases. Although light propagation and backscattering within tissues are a complicated physical process in the presence of pathologies, the published strategy by Zhang and associates,[18] in which the inverted structural image derived from the CC slab is used to compensate for the intensity of CC flow image, works well for drusen. Specific examples of the application of this approach on eyes with drusen can be found in previous publications.[19,20] This strategy also compensates for the lack of uniformity in the OCT signal across the scan area. This approach requires an accurate CC slab, as defined earlier in this study. For inaccurate slabs that are deeper into the choroid, especially ones with variegated appearances in the OCT *en face* images, brighter signals from pigments in deeper choroid in the structural image could introduce unwanted artifacts.[21] This approach has its limitations; for example, signals of areas underneath migrated pigments might be beyond salvation and should be excluded. Different compensation strategies might be needed for other pathologies, such as retinal edema or hyper-reflective materials located above the retinal pigment epithelium/BM complex. Finally, retinal projection artifacts[22] need to be removed for optimal imaging of the CC before any quantitation is performed.

ACCURATE CC QUANTIFICATION USING OCTA

ONCE GOOD VISUALIZATION OF THE CC IS OBTAINED, THE next steps will ensure accurate quantitation of CC parameters using OCTA.

• **MEASURED ICDS SHOULD BE CONSISTENT WITH KNOWN MEASUREMENTS USING HISTOLOGY:** An important quantitative parameter that researchers should consider when dealing with OCTA CC images is the ICD. The ICD is defined as the averaged distance from the center of one capillary lumen to another. Therefore, it is substantially equivalent to 1 capillary width plus the width of 1 physiological flow void. In some histological studies, the ICD was defined as the distance from the edge of 1 capillary to another.[16] Multiple groups reported measurements of ICD values using a radially averaged power spectrum analysis with different OCTA systems.[12–14,17,23] This measurement is performed by generating and radially averaging a 2-dimensional power spectrum from OCTA CC images. The resultant peak in the averaged plot represents the most prevalent spacing, which is the averaged ICD in the CC images. Previous histological studies[16] reported that in macular regions the CC vessel diameter is approximately 16-20 μm, whereas the vessel edge-to-edge distance is 5-20 μm. Thus, according to the previous definition of ICD, 1 vessel width plus 1 flow void width would provide an ICD of approximately 21-40 μm. Due to the limitations of OCTA, the calculated ICDs might not match with the histological measurements exactly but should be relatively consistent with this 21-40 μm range. This ICD measurement does not require a binarization algorithm.

• **SELECTED PARAMETERS MUST BE PHYSIOLOGICALLY AND PHYSICALLY MEANINGFUL:** As previously discussed, the limited lateral resolution of OCTA images makes it difficult to visualize the detailed macular CC vasculature network.[5] Instead of developing a binarization algorithm to segment individual capillaries, most researcher choose to segment flow deficits (FDs), which can be larger than the typical size of physiological flow voids, are within the detection sensitivity of OCTA images, and represent CC flow impairment, which is the feature of the CC that is associated with disease. Many quantitative parameters have been introduced in various reports[17,24,25] to describe CC FDs, but it is important for researchers to only select parameters that are physiologically and physically meaningful. Some appropriate metrics include FD density (FDD), FD number, mean FD size, or average FD size/average FD area and ICD. Some inappropriate parameters include vessel skeleton density, vessel length density, and vessel diameter index. Generally speaking, researchers should avoid using any parameter that involves skeletonizing the binarized CC image unless they can prove that individual CC vessels have been fully resolved and segmented in their images. With the current OCTA lateral resolution, we can only reasonably attempt to measure the perfusion deficits within the CC (or FDs) but not with detailed vascular morphology patterns.

• **SELECTED ALGORITHM FOR CC BINARIZATION MUST BE APPROPRIATE AND GENERATE MEANINGFUL RESULTS:** To quantify the previously mentioned meaningful parameters, the OCTA CC images must be binarized, which requires applying a thresholding strategy. Several thresholding algorithms have been used in the literature to segment the CC FDs. As we discussed in a previous publication, some of those algorithms were not appropriate to the task at hand for various reasons.[5] Useful methods that are available include: 1) a global thresholding method that uses SD values of a normal database (SD method)[18]; 2) a thresholding method that uses the fuzzy C-means algorithm (FCM method)[17]; and 3) the Phansalkar local thresholding method (Phansalkar method).[26] We previously reported a high correlation between the SD method and the FCM method using a normative database.[27] Moreover, we also pointed out that when using the Phansalkar method, the choice of local window radius can significantly affect the appearance of binarized CC FD images and subsequent quantification.[5] Many researchers[26,28–30] used a fixed 15-pixel radius window with the Phansalkar method, although, due to the properties of the various scan patterns, the actual pixel size ranged from 2.9 to 9.9 μm/pixel in these studies. The discrepancy in the physical dimensions of the window radius was particularly concerning, and this discrepancy compromised the assessment of previously published reports and made cross validation comparisons difficult.

To explore how the choice of different window radii influences CC quantification, we conducted a study[19] in which eyes scanned using a SS-OCTA instrument (PLEX Elite 9000, Carl Zeiss Meditec) were analyzed using the Phansalkar method, with window radii ranging from 1 to 15 pixels (3 × 3 mm: 2.9 μm/pixel, 6 × 6 mm: 5.9 μm/pixel for images adjusted to 1,024 × 1,024 pixels). In our study, we found that larger window radii resulted in higher FDD values. With the increase in the window size, the FD number initially increased and then decreased, and the opposite trend was found for mean FD size. However, the inflection point for this change corresponded to a window radius equal to approximately 1-2 ICDs, which provided some justification for considering this to be an optimal choice for the proper use of the Phansalkar method. Moreover, this choice of 1-2 ICDs for the window radius yielded images that closely resembled the actual CC flow images before binarization and were substantially indistinguishable from the results obtained using the FCM approach, as demonstrated in Figure 5. After analyzing our data, we concluded the Phansalkar method could be a good approach for the CC quantification, as long as its

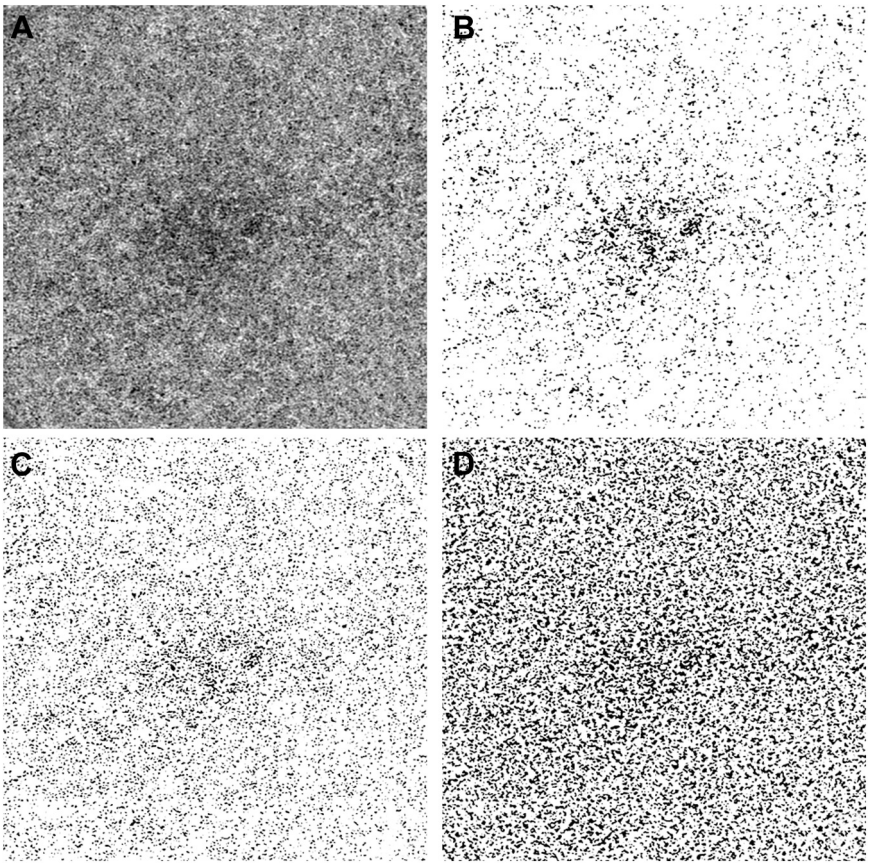

FIGURE 5. Comparison of choriocapillaris (CC) flow deficits (FDs) segmented using different algorithms with PLEX Elite 9000 swept-source optical coherence tomography angiography (SS-OCTA). (A) 6 × 6-mm *en face* SS-OCTA CC image from a normal eye (1,024 × 1,024 pixels). (B) Segmented CC FDs binary map using the Fuzzy C-means method; black pixels represent FDs. (C) Segmented CC FDs binary map using the Phansalkar local thresholding method, with a window radius of 3 pixels (a diameter of 41 μm). (D) Segmented CC FDs binary map using the Phansalkar local thresholding method, with a window radius of 15 pixels (a diameter of 182 μm).

parameters, especially the local window radius, were optimized for the OCTA CC images. Therefore, we recommend that the proper use of the Phansalkar method should include the selection of the window radius related to the expected ICD in normal eyes. Thus, for the Phansalkar method, 1-2 ICDs should be selected as the window diameter (2 × radius + 1 pixels), then for a 3 × 3-mm scan (2.9 μm/pixel), a radius of 4-8 pixels could be chosen, and for a 6 × 6-mm scan (5.9 μm/pixel), a radius of 2-4 pixels could be chosen. In the case of CC binarization, it is clear that global thresholding techniques and local thresholding techniques each have its own merits and limitations. Future studies may also consider using >1 binarization technique to ensure accurate evaluation.

As mentioned previously, when developing an algorithm for CC binarization, the most straightforward criterion for judging the validity of any binarization strategy is to compare the OCTA CC flow image side-by-side with the binarized CC FD image. The major FDs segmented in the binarized image should closely resemble the FDs in the original OCTA CC image. The binarized CC FD image should not appear to create false positive FDs or artificial vasculature networks. Moreover, the calculated CC FD quantitative parameters should stay consistent with histological studies. Because OCT imaging is a convolutional process with a lateral resolution of approximately 20 μm (imaged features will be dilated ~20 μm larger), the CC imaged by OCTA appears wider. Consequently, the CC perfusion density calculated from OCTA images should be expected to be considerably larger than the values calculated from histological images. Taking quantification of retinal vasculature as an example, a previous histological study that used confocal scanning laser microscopy reported on vessel area density, which is the opposite of the flow deficit density, in the ganglion cell—inner plexiform layer, as 22.32% ± 0.99%,[31] whereas this value was 48.6% ± 1.4% from the OCTA assessment.[32] This significant difference in reported vessel density was mainly caused by lateral resolution of OCTA. Similarly, CC density (which is equal to 1.0 FDD) measured by OCTA should also result in higher

values compared with the CC density measured by histological studies,[10] meaning that OCTA-measured FDD should be lower than the real values. If abnormally high FDD values are obtained using OCTA, it is possible that the selected thresholding technique has not been optimized.

Most studies have adopted a signal strength cutoff as part of their data inclusion criterion, per the recommendations of OCTA manufacturer. However, studies have also shown positive correlation in the signal strength with quantitative vasculature metrics, even above the common cutoffs.[33,34] Therefore, it might be useful to adopt a signal normalization strategy in CC quantification. Zhang and associates[22] previously normalized data with a signal strength index of <9 against an index of 9, in which each voxel in the OCT and OCTA volume was multiplied by a factor of 9 divided by the actual signal strength index of the data, before segmentation and *en face* image generation took place. Such strategy might not work perfectly because it is unknown how device manufacturers defined their signal strength index. For future work, it might be necessary for the device manufacturers to become involved in the signal normalization to obtain more accurate CC quantifications.

• **MULTIPLE SCANS OF SAME SIZE AND DIFFERENT SIZES SHOULD BE REPEATABLE AND CORRELATED:** Researchers should make sure that their quantitative analyses of the CC demonstrate repeatability in both normal and diseased eyes. If the OCTA CC flow metrics are to be used as a biomarker for assessing disease pathology and progression, then quantitative CC metrics should be able to demonstrate good repeatability. Otherwise, it would be simply impossible to compare CC properties among patient cohorts or track disease progression. Quantitative metrics acquired from the multiple scans of the same subjects using the same scanning pattern should have good repeatability. Likewise, quantitative metrics acquired from multiple scans of the same subjects using different scanning patterns (3 × 3 mm and 6 × 6 mm) should be highly correlated.[35] Various studies have used coefficient of variation and intraclass correlation coefficient values[18] to judge the clinical usefulness of results. When publishing new studies with new quantification approaches, it is important that researchers investigate the reproducibility properties and compare them to those of other algorithms. Most importantly, high repeatability should not be obtained at the cost of sensitivity. For quantitative CC metrics to be used as biomarkers, researchers must demonstrate both high repeatability of measurements as well as high sensitivity in detecting pathology; high repeatability of any given measurement is not a substitute for sensitivity.[6] Because a particular slab yields results that are repeatable does not mean that the results are relevant for detecting disease. Researchers need to assess the relationship between repeatability and sensitivity.

OCTA systems typically provide multiple choices of scanning patterns. For example, in the current SS-OCTA instrument (PLEX Elite 9000), options include 3 × 3 mm, 6 × 6 mm, 9 × 9 mm, 9 × 15 mm, and 12 × 12 mm scan patterns. However, not all scans are suitable for the CC quantification. Because of the limited lateral resolution of the system, it is best to use images that sample the retina tissue as densely as possible. The 3 × 3 mm scan has a sampling (or scanning) density of 10 μm/pixel, and the 6 × 6 mm scan has a sampling density of 12 μm/pixel. Both scan sizes have been reported to be useful in the quantitative CC analyses. However, larger scans such as 9 × 9 mm, 9 × 15 mm and 12 × 12 mm scans currently use a larger sampling density of 18 μm/pixel and 24 μm/pixel, making it almost impossible to provide reliable quantitative assessment of the CC network. The thickness measurements of the retinal pigment epithelium, BM and CC layers also vary between the macular region to the equatorial regions.[36] Therefore, variegated appearances of CC OCT structural images from larger scans can be observed when a uniformly defined CC slab is used. This often indicates inaccurate CC visualization with larger scanning patterns.

SUMMARY AND FUTURE CONSIDERATIONS

THERE ARE NUMEROUS ISSUES TO BE CONSIDERED WHEN IMaging the CC with OCTA and carrying out a quantitative analysis of such images. In our pursuit of an optimal protocol to tackle this problem, we have made some mistakes and learned many lessons. In this report, we presented a summarized checklist of how best to visualize and quantify the CC with OCTA. In each claim, we presented specific guidelines, as well as provided rationale and evidence.

In summary, we argue that to achieve an accurate and reliable CC quantitative analysis using OCTA, researchers must make sure that both the visualization of the CC and the quantification of the CC are physically and physiologically justifiable. As a first step to ensure accurate visualization of the CC, the selection of the CC slab must be physiologically sound. The CC slab should be defined as a 10-20 μm thickness slab beneath the BM. Proprietary algorithms from manufactures or various research groups most often define the CC slab by segmenting either the retinal pigment epithelium or BM. With such approaches, the difference offset from the segmentation line may depend on the specific characteristics of the segmentation and should be decided using retinal pigment epithelium and BM thicknesses calculated from histological studies.[10,11] A CC slab could also be segmented by using averaged A-lines to identify the BM and the posterior boundary of the CC. Averaged OCT A-lines could be used to identify the position of the BM, and the anterior boundary of the CC should be approximately 2-4 μm below

this BM position. Averaged OCTA A-lines could be used to identify the posterior boundary of the CC. When defining the CC slab, the OCT structural CC *en face* image should always be examined to avoid a variegated appearance caused by irregular structures in the deeper choroid. The generated OCTA CC images should show a similar appearance to histology. OCTA CC images under the macula should have a dense meshwork appearance, whereas in the equatorial region, the CC images should have more lobular pattern. Finally, multiple OCTA CC images from the same and different scan sizes should be qualitatively similar.

Once a good visualization of the CC is achieved, the additional steps are necessary to ensure accurate CC quantification. If researchers choose to measure the ICD, it should be consistent with known measurement using histology (~21-40 μm).[16] If researchers choose to segment and quantify FDs, the selected parameters must be physiologically and physically meaningful. Parameters like vessel skeleton density, vessel length density, and vessel diameter index should be avoided due to the inability to resolve individual CC vessels, at least in the submacular region, using current SS-OCTA systems. In the process of segmenting the CC FDs, the selected algorithm for CC binarization must be appropriate and generate physically meaningful results. If the Phansalkar method is chosen, its parameters should be optimized using a window radius that is specific for the OCTA CC images. We recommend using a window radius of 1-2 ICDs. Finally, quantitative metrics generated by the multiple scans of the same and different sizes should be repeatable and correlated.

The limited lateral resolution of OCTA is the most important reason why the quantitative analysis of the CC is so complicated. Quite simply, it is difficult to confirm accurate visualization and quantification of the CC in the macula where the imaging technology is unable to resolve the detailed microvascular network. However, this does not mean that the commercially available OCTA instruments are not useful in CC analysis. Although OCTA cannot always resolve individual CC vessels, it is typically capable of resolving the lack of CC flow, which is why we choose to segment and quantify CC FDs instead of actual vessels. Currently, efforts have begun to develop next-generation instruments that will achieve higher resolution and faster speeds for CC imaging.[13,37] It is possible that with the technological advancements, commercial OCTA systems could achieve the ability to make CC imaging more straightforward and easier to quantitate in the future. However, for now, we strongly encourage researchers to follow the guidelines provided in this perspective so they can generate meaningful quantitative CC metrics that are similar across platforms to help diagnose, follow, and predict the progression of ocular diseases.

CRediT AUTHORSHIP CONTRIBUTION STATEMENT

ZHONGDI CHU: CONCEPTUALIZATION, METHODOLOGY, Software, Visualization, Investigation, Writing - original draft, Writing - review & editing. **Qinqin Zhang:** Data curation, Software, Writing - review & editing. **Giovanni Gregori:** Resources, Conceptualization, Writing - review & editing, Funding acquisition. **Philip J. Rosenfeld:** Resources, Conceptualization, Writing - review & editing, Funding acquisition. **Ruikang K. Wang:** Resources, Conceptualization, Writing - review & editing, Funding acquisition.

ALL AUTHORS HAVE COMPLETED AND SUBMITTED THE ICMJE FORM FOR DISCLOSURE OF POTENTIAL CONFLICTS OF interest. Funding/support: This research was supported by grants from the National Eye Institute (R01EY024158, R01EY028753, R01AG060942), the Salah Foundation, Carl Zeiss Meditec, an unrestricted grant from the Research to Prevent Blindness, Inc., and the National Eye Institute Center Core Grant (P30EY014801) to the Department of Ophthalmology, University of Miami Miller School of Medicine.

Financial disclosures: Drs. Gregori, Wang, and Rosenfeld received research support from Carl Zeiss Meditec, Inc. Dr. Gregori and the University of Miami co-own a patent that is licensed to Carl Zeiss Meditec, Inc. Dr. Rosenfeld has received research support from Stealth BioTherapeutics; has been a consultant for Apellis, Biogen, Boehringer-Ingelheim, Carl Zeiss Meditec, Biogen, Chengdu Kanghong Biotech, EyePoint, Ocunexus Therapeutics, Ocudyne, and Unity Biotechnology; and holds equity interest in Apellis, Valitor, Verana Health, and Ocudyne. Dr. Wang has received research support from Tasso Inc, Moptim Inc, Colgate Palmolive Company and Facebook technologies LLC; has been a consultant to Insight Photonic Solutions, Kowa, and Carl Zeiss Meditec. The other authors have reported that they have no relationships relevant to the contents of this paper to disclose.

REFERENCES

1. Lutty G, Grunwald J, Majji AB, Uyama M, Yoneya S. Changes in choriocapillaris and retinal pigment epithelium in age-related macular degeneration. *Mol Vis* 1999;5(35):35.
2. Cao J, McLeod DS, Merges CA, Lutty GA. Choriocapillaris degeneration and related pathologic changes in human diabetic eyes. *Arch Ophthalmol* 1998;116(5):589–597.
3. Spraul CW, Lang GE, Lang GK, Grossniklaus HE. Morphometric changes of the choriocapillaris and the choroidal vasculature in eyes with advanced glaucomatous changes. *Vision Res* 2002;42(7):923–932.
4. Piccolino FC, Borgia L. Central serous chorioretinopathy and indocyanine green angiography. *Retina* 1994;14(3):231–242.
5. Chu Z, Gregori G, Rosenfeld PJ, Wang RK. Quantification of choriocapillaris with OCTA: a comparison study. *Am J Ophthalmol* 2019;208:111–123.

6. Byon I, Nassisi M, Borrelli E, Sadda SR. Impact of slab selection on quantification of choriocapillaris flow deficits by optical coherence tomography angiography. *Am J Ophthalmol* 2019;208:397–405.
7. Mehta N, Liu K, Alibhai AY, et al. Impact of binarization thresholding and brightness/contrast adjustment methodology on optical coherence tomography angiography image quantification. *Am J Ophthalmol* 2019;205:54–65.
8. Yin X, Chao JR, Wang RK. User-guided segmentation for volumetric retinal optical coherence tomography images. *J Biomed Opt* 2014;19(8):086020.
9. Torczynski E, Tso MO. The architecture of the choriocapillaris at the posterior pole. *Am J Ophthalmol* 1976;81(4):428–440.
10. Ramrattan RS, van der Schaft TL, Mooy CM, De Bruijn W, Mulder P, De Jong P. Morphometric analysis of Bruch's membrane, the choriocapillaris, and the choroid in aging. *Invest Ophthalmol Vis Sci* 1994;35(6):2857–2864.
11. Spraul CW, Lang GE, Grossniklaus HE. Morphometric analysis of the choroid, Bruch's membrane, and retinal pigment epithelium in eyes with age-related macular degeneration. *Invest Ophthalmol Vis Sci* 1996;37(13):2724–2735.
12. Gorczynska I, Migacz J, Jonnal R, Zawadzki R, Poddar R, Werner J. Imaging of the human choroid with a 1.7 MHz A-scan rate FDML swept source OCT system. Ophthalmic Technologies XXVII: International Society for Optics and Photonics, 10045. San Francisco, California, United States: Event, SPIE BiOS; 2017:1004510. https://doi.org/10.1117/12.2251704.
13. Zhou K, Song S, Zhang Q, Chu Z, Huang Z, Wang RK. Visualizing choriocapillaris using swept-source optical coherence tomography angiography with various probe beam sizes. *Biomed Opt Express* 2019;10(6):2847–2860.
14. Kurokawa K, Liu Z, Miller DT. Adaptive optics optical coherence tomography angiography for morphometric analysis of choriocapillaris. *Biomed Opt Express* 2017;8(3):1803–1822.
15. Yoneya S, Tso MO, Shimizu K. Patterns of the choriocapillaris. *Int Ophthalmol* 1983;6(2):95–99.
16. Olver J. Functional anatomy of the choroidal circulation: methyl methacrylate casting of human choroid. *Eye* 1990;4(2):262–272.
17. Chu Z, Zhou H, Cheng Y, Zhang Q, Wang RK. Improving visualization and quantitative assessment of choriocapillaris with swept source OCTA through registration and averaging applicable to clinical systems. *Sci Rep* 2018;8(1):16826.
18. Zhang Q, Zheng F, Motulsky EH, et al. A novel strategy for quantifying choriocapillaris flow voids using swept-source OCT angiography. *Invest Ophthalmol Vis Sci* 2018;59(1):203–211.
19. Chu Z, Cheng Y, Zhang Q, et al. Quantification of choriocapillaris with Phansalkar local thresholding: pitfalls to avoid. *Am J Ophthalmol* 2020;213:161–176.
20. Shi Y, Chu Z, Wang L, et al. Validation of a compensation strategy used to detect choriocapillaris flow deficits under drusen with swept source OCT angiography. *Am J Ophthalmol* 2020;220:115–127.
21. Ledesma-Gil G, Fernandez-Avellaneda P, Spaide RF. Swept-source optical coherence tomography angiography image compensation of the choriocapillaris induces artifacts. *Retina* 2020;40(10):1865–1872.
22. Zhang Q, Zhang A, Lee CS, et al. Projection artifact removal improves visualization and quantitation of macular neovascularization imaged by optical coherence tomography angiography. *Ophthalmol Retina* 2017;1(2):124–136.
23. Zhang Q, Shi Y, Zhou H, et al. Accurate estimation of choriocapillaris flow deficits beyond normal intercapillary spacing with swept source OCT angiography. *Quant Imag Med Surg* 2018;8(7):658.
24. Sacconi R, Borrelli E, Corbelli E, et al. Quantitative changes in the ageing choriocapillaris as measured by swept source optical coherence tomography angiography. *Br J Ophthalmol* 2019;103(9):1320–1326.
25. Uji A, Balasubramanian S, Lei J, Baghdasaryan E, Al-Sheikh M, Sadda SR. Choriocapillaris imaging using multiple en face optical coherence tomography angiography image averaging. *JAMA Ophthalmol* 2017;135(11):1197–1204.
26. Spaide RF. Choriocapillaris flow features follow a power law distribution: implications for characterization and mechanisms of disease progression. *Am J Ophthalmol* 2016;170:58–67.
27. Chu Z, Zhang Q, Zhou H, et al. Quantifying choriocapillaris flow deficits using global and localized thresholding methods: a correlation study. *Quant Imag Med Surg* 2018;8(11):1102.
28. Nassisi M, Baghdasaryan E, Tepelus T, Asanad S, Borrelli E, Sadda SR. Topographic distribution of choriocapillaris flow deficits in healthy eyes. *PloS One* 2018;13(11):e0207638.
29. Nassisi M, Shi Y, Fan W, et al. Choriocapillaris impairment around the atrophic lesions in patients with geographic atrophy: a swept-source optical coherence tomography angiography study. *Br J Ophthalmol* 2019;103(7):911–917.
30. Spaide RF. Ising model of choriocapillaris flow. *Retina* 2018;38(1):79–83.
31. Chan G, Balaratnasingam C, Paula KY, et al. Quantitative morphometry of perifoveal capillary networks in the human retina. *Invest Ophthalmol Vis Sci* 2012;53(9):5502–5514.
32. Richter GM, Madi I, Chu Z, et al. Structural and functional associations of macular microcirculation in the ganglion cell-inner plexiform layer in glaucoma using optical coherence tomography angiography. *J Glaucoma* 2018;27(3):281–290.
33. Brücher VC, Storp JJ, Eter N, Alnawaiseh M. Optical coherence tomography angiography-derived flow density: a review of the influencing factors. *Graef Arch Clin Exp Ophthalmol* 2020;258(4):701–710.
34. Lim HB, Kim YW, Kim JM, Jo YJ, Kim JY. The importance of signal strength in quantitative assessment of retinal vessel density using optical coherence tomography angiography. *Sci Rep* 2018;8(1):1–8.
35. Zheng F, Zhang Q, Shi Y, et al. Age-dependent changes in the macular choriocapillaris of normal eyes imaged with swept-source optical coherence tomography angiography. *Am J Ophthalmol* 2019;200:110–122.
36. Spraul CW, Lang GE, Grossniklaus HE, Lang GK. Histologic and morphometric analysis of the choroid, Bruch's membrane, and retinal pigment epithelium in postmortem eyes with age-related macular degeneration and histologic examination of surgically excised choroidal neovascular membranes. *Surv Ophthalmol* 1999;44:S10–S32.
37. Marsh-Armstrong B, Migacz J, Jonnal R, Werner JS. Automated quantification of choriocapillaris anatomical features in ultrahigh-speed optical coherence tomography angiograms. *Biomed Opt Express* 2019;10(10):5337–5350.